DOI: 10.1002/chem.200800802

Rubrenes: Planar and Twisted

Abhimanyu S. Paraskar,[a] A. Ravikumar Reddy,[a] Asit Patra,[a] Yair H. Wijsboom,[a] Ori Gidron,[a] Linda J. W. Shimon,[b] Gregory Leitus,[b] and Michael Bendikov*[a]

Abstract: Surprisingly, despite its very high mobility in a single crystal, rubrene shows very low mobility in vacuum-sublimed or solution-processed organic thin-film transistors. We synthesized several rubrene analogues with electron-withdrawing and electron-donating substituents and found that most of the substituted rubrenes are not planar in the solid state. Moreover, we conclude (based on experimental and calculated data) that even parent rubrene is not planar in solution and in thin films. This discovery explains why high mobility is reported in rubrene single crystals, but rubrene shows very low field-effect mobility in thin films. The substituted rubrenes obtained in this work have significantly better solubility than parent rubrene and some even form films and not crystals after evaporation of the solvent. Thus, substituted rubrenes are promising materials for organic light-emitting diode (OLED) applications.

Keywords: field-effect transistors · materials science · organic electronic materials · rubrenes · substituent effects

Introduction

Rubrene (5,6,11,12-tetraphenyltetracene; **1**) has been known since the beginning of the last century.[1] The electroluminescence and chemiluminescence of **1** were well studied in the 1960s and it is a classic example of a material with excellent electrochemiluminescent properties.[2] Nowadays, compound **1** is used as a dopant and a photosensitizer in organic light-emitting diodes (OLEDs). Recently, compound **1** was investigated as an active semiconductor in organic field-effect transistors (OFETs).[3] An exceptionally high field-effect mobility of up to 15 $cm^2 V^{-1} s^{-1}$ was measured for single crystals of **1**,[4] and later, a contact-free intrinsic mobility of 40 $cm^2 V^{-1} s^{-1}$ was reported for **1**.[5,6] Surprisingly, despite its very high mobility in a single crystal, compound **1** shows very low mobility in vacuum-sublimed or solution-processed organic thin-film transistors.[7,8] To overcome this problem, thin films based on crystalline mixtures of 5,12-diphenylanthracene and **1** were prepared, with these reported to yield a hole mobility of up to 0.7 $cm^2 V^{-1} s^{-1}$,[8] and transistor arrays based on single crystals of **1**[9] were also fabricated.[10,11]

Apparently, good crystal packing is responsible for the observed high mobility,[12] and indeed, examination of the crystal structure of **1**[13] shows that it has π–π stacking in one direction and a herringbone motif in another direction. The molecular structure of **1** consists of an absolutely planar tetracene backbone in the solid state,[13] although very similar molecules were found to be twisted.[14,15] In the X-ray structure of rubrene, significant steric repulsion between the phenyl rings shifts them above and below the tetracene plane forming a dihedral angle of 25°. The tetracene core is still practically planar, thus steric repulsion between the phenyl rings is balanced by the rigidity of the tetracene core. Even large twisting of the acene backbone does not change the HOMO–LUMO gap of acenes significantly.[16] On the other hand, the energy required for twisting acenes by 10–20° is only a few $kcal\,mol^{-1}$, however, it increases to 40 $kcal\,mol^{-1}$ for twisting more than 80°.[16,17] Recently, the supramolecular self-assembly of **1** on an Au(111) surface was studied by STM and other methods.[18]

---

[a] Dr. A. S. Paraskar,[#] Dr. A. R. Reddy,[#] Dr. A. Patra,[#] Y. H. Wijsboom,
O. Gidron, Dr. M. Bendikov
Department of Organic Chemistry
Weizmann Institute of Science
Rehovot 76100 (Israel)
Fax: (+972) 8934-4142
E-mail: michael.bendikov@weizmann.ac.il

[b] Dr. L. J. W. Shimon, Dr. G. Leitus
Chemical Research Support Unit
Weizmann Institute of Science
Rehovot 76100 (Israel)

[#] These authors contributed equally to the work.

Supporting information for this article is available on the WWW under http://dx.doi.org/10.1002/chem.200800802.

Despite great interest in **1** in materials science, very few substituted rubrenes are known[19] and the electronic and structural properties of substituted rubrenes have never been studied. The parent rubrene (**1**) is also only modestly soluble in organic solvents. Our original motivation was to design rubrene derivatives suitable for thin film transistors by improving charge mobility and solubility by appropriate chemical substitution. To this end, we synthesized several rubrene analogues **2**–**7** (Scheme 1) with electron-withdrawing and electron-donating substituents and found that most of the substituted rubrenes are not planar in the solid state. Moreover, we conclude that even **1** is not planar in solution nor, most probably, in thin films. This discovery explains why high mobility is reported in single crystals of **1**, but **1** does not show any field-effect mobility in conventional thin films. The substituted rubrenes obtained in this work have significantly better solubility than **1** and some even form films and not crystals after evaporation of the solvent. Thus, substituted rubrenes are promising materials for OLED applications.

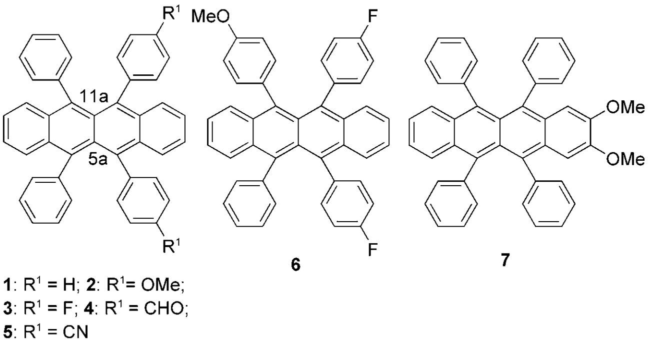

Scheme 1. Structure of rubrenes **1**–**7** synthesized in this work.

Results and Discussion

Synthesis of rubrenes 1–7: Rubrenes **1** and **2** were synthesized according to a literature procedure.[19a] Rubrenes **3**–**7** were prepared from the corresponding 6,11-diaryltetracene-5,12-diones (**11**–**13**) by using aryllithiums or Grignard reagents followed by HI-mediated aromatization of the corresponding diols (**16**–**20**; Scheme 2).

Nucleophilic addition of **11** and 4-fluorophenylmagnesium bromide, prepared from 1-bromo-4-fluorobenzene and *i*PrMgCl•LiCl,[20] was carried out in THF under an inert atmosphere to give **16**. HI-promoted aromatization of **16** provided rubrene **3** as a red solid. Quinone **11** was treated with 4-bromobenzaldehyde diethyl acetal in the presence of BuLi in THF to obtain **17** followed by aromatization with HI in diethyl ether at reflux to give rubrene **4** as a red solid. Similarly, cyano-substituted rubrene **5** was prepared in a good yield (Scheme 2).

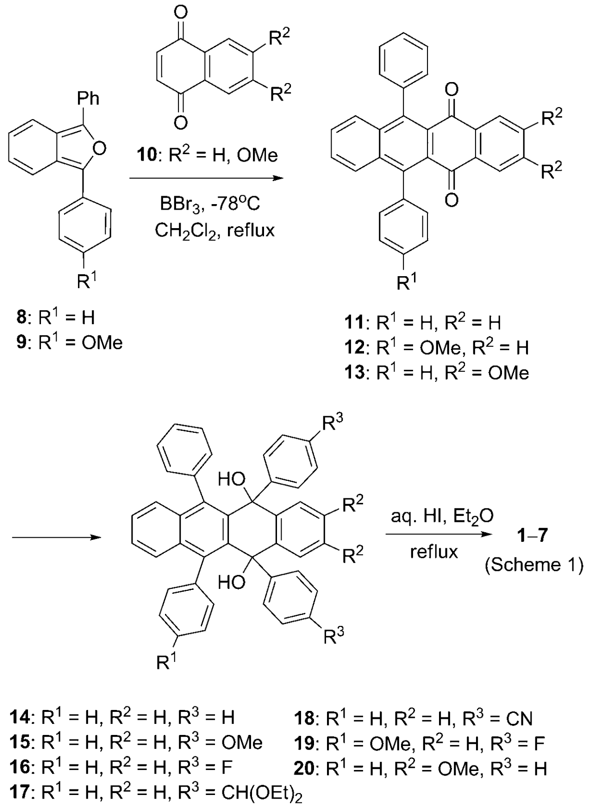

Scheme 2. Synthesis of rubrenes **1**–**7**. See text for a description of the conversion of **11**–**13** into **14**–**20**.

To prepare monomethoxydifluoro-substituted rubrene **6**, methoxy-substituted isobenzofuran **9** was prepared in two steps from commercially available 3-phenylpthalide by addition of 4-methoxyphenyllithium and subsequent dehydration with acetic anhydride. A cycloaddition reaction between **9** and 1,4-naphthaquinone gave quinone **12**. Quinone **12** was treated with 1-bromo-4-fluorobenzene in the presence of *n*BuLi to provide **19**, which was treated with HI in diethyl ether to give the rubrene **6**. Introduction of methoxy group in the tetracene core of rubrene was achieved by treating 1,3-diphenyisobenzofuran (**8**) with **10** (R^2 = OMe) to give **13**. Quinone **13** was treated with phenyllithium to provide **20**, which was subjected to aromatization to give rubrene **7** (Scheme 2). Rubrenes **1**–**7** were purified by sublimation before characterization (in addition to column chromatography as described in the Experimental Section).

X-ray crystal structures: Single crystals of rubrenes **2**, **3**, **4**, and **6** were grown from a mixture of dichloromethane and ethanol. Unexpectedly, the X-ray structure of **2** shows that the molecule adopts a strongly twisted conformation with approximately D_2 symmetry (Figures 1 and 2).[21] The end-to-end twist of the tetracene core is 44.0°. The twist is unevenly distributed with the four tetracene rings contributing 4.8, 15.6, 16.2, and 7.4° to the twist. X-ray structures of all twisted rubrenes examined in this paper form centrosymmetric crystals in which the same number of right- and left-twisted molecules (both enantiomers) are present. On the other hand, the X-ray structure of difluoro-substituted rubrene **3** adopts a planar conformation very similar to that of **1**. The fact that some acene-type molecules adopt different conformations (planar and twisted) depending on the substituents has been previously observed for substituted naphthalenes and benzannulated anthracenes.[22] Interestingly, crystals of **1** and **3** are isostructural with almost the same unit cell parameters

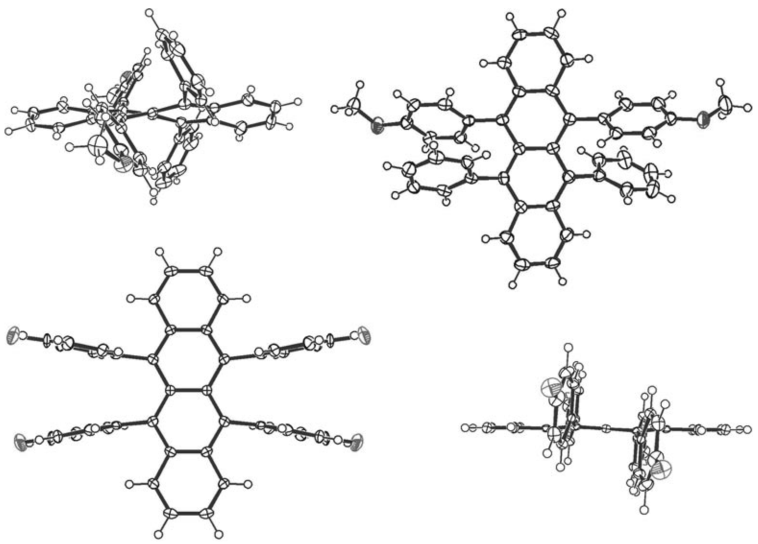

Figure 1. Crystal structures of **2** (top, showing the twist around the tetracene core) and **3** (bottom, showing the planarity of the tetracene core).

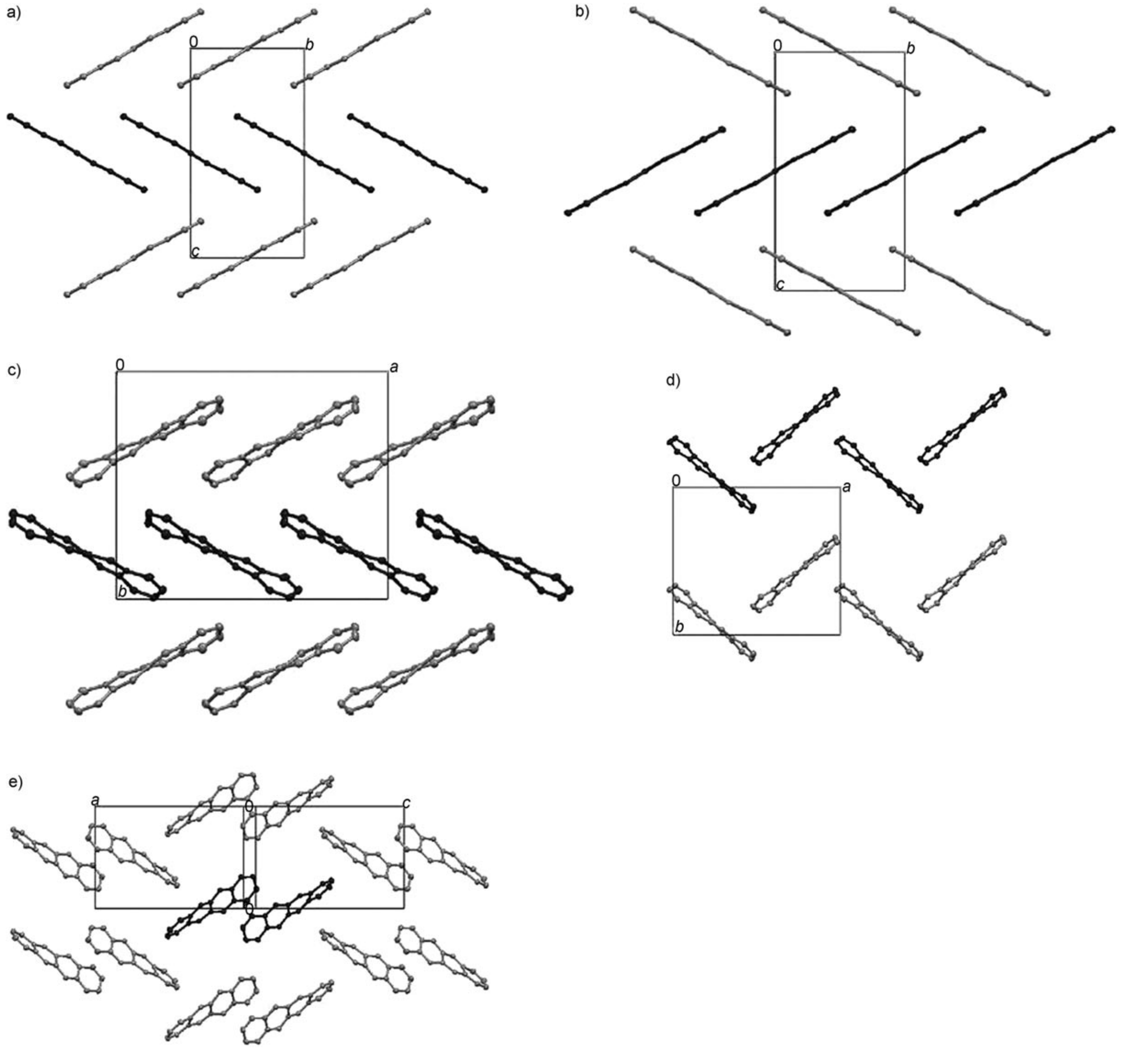

Figure 2. Packing arrangements of a) **1**, b) **3**, c) **2**, d) **4**, and e) **6**. Only tetracene cores are shown for clarity.

except for the *a* lattice dimension, which is longer in **3**. The X-ray structures of **6** (with both difluoro and methoxy groups), for which the end-to-end twist of the tetracene core is 35.2°, and of diformyl **4**, for which the end-to-end twist of the tetracene core is 37.7°, are similar to that of **2**. However, crystal structures of **2**, **3**, **4**, and **6** have different packing arrangements (Figure 2). Twisting of the tetracene core results in worse crystal packing relative to the rubrenes with a planar tetracene core (as indicated by a lower packing index[23]) and consequently leads to weaker intermolecular interactions. As a result, twisted rubrenes are not good candidates for applications in OFET. Based on solid-state X-ray structures of **1** and substituted rubrenes, we have shown that the solid-state structures, and consequently, the properties of rubrenes can be modified by substitution.

Computational results: The planar (C_{2h} symmetry) structure of rubrene lies 3.8 kcal mol^{-1} higher in energy than the minimum structure (D_2 symmetry) for which the tetracene core is highly twisted by 42° (at the B3LYP/6-31G(d) level of theory).[23,24,25] The planar D_{2h} structure of rubrene is a second-order saddle point lying 6.5 kcal mol^{-1} above the minimum-energy structure. Interestingly, neither donor nor acceptor substituents on the phenyl rings change the twisting or planarization energies. Thus, in compounds **2** and **5**, the twisting angles are 43.2 and 42.3°, respectively, with the planar structures (C_s symmetry) lying 4.0 and 3.6 kcal mol^{-1} higher in energy, respectively. So, twisting of the central tetracene core in rubrene does not result from an electronic effect of the phenyl ring substituents.

In solution, even **1** has a twisted structure based on a comparison of the measured and calculated (GIAO-B3LYP/6-311G(2df,p)//B3LYP/6-31G(d)) ^{13}C NMR spectroscopy values, with the latter corrected for the chemical shifts of 9,10-diphenyl anthracene.[23] The average difference between the measured NMR chemical shifts of the carbon atoms of the tetracene core and the shifts calculated for a twisted conformation (by using the minimum-energy structure) is 0.46 ppm, whereas this difference is significantly larger (1.85 ppm) if the measured shifts are compared with shifts calculated for planar rubrene.[23] The difference in the calculated chemical shifts of the central quaternary carbon atoms of the tetracene core (carbon atoms 5a and 11a, Scheme 1) for the planar and twisted structure is especially pronounced, while all other carbon atoms are less sensitive to twisting. Calculated values for carbon atoms 5a and 11a in a twisted conformation are just 0.3 ppm off the measured values, whereas the difference between the experimental and calculated values is 4.0 ppm for a planar conformation.[23,26] We can conclude that the rubrene molecules are intrinsically nonplanar and steric repulsions are responsible for twisting in rubrenes, whereas crystal-packing forces are responsible for the planar tetracene core observed in the crystals of **1** and **3**. Based on these data, a nonplanar geometry is expected for rubrene and its derivatives in conventional thin films.

UV/Vis absorption and emission spectroscopy: The absorption and emission data for all substituted rubrenes are summarized in Table 1. The UV/Vis absorption ($\lambda_{\text{max,abs}}$ = 520–529 nm) and emission ($\lambda_{\text{max,ems}}$ = 553–568 nm) spectra are very similar for all substituted rubrenes (Figure 3). In solution, the effect of the phenyl ring substituents on the electronic properties of rubrene is small. Substituted rubrenes are strongly fluorescent, some with a quantum yield of close to 100 %. The quantum yields for rubrene analogues with methoxy-substituted phenyl rings (**2** and **6**) are relatively

Table 1. Optical properties of substituted rubrenes **1**–**7**.

	$\lambda_{\text{max,abs}}$ [nm]	$\varepsilon_{\lambda\text{max}}$ [M^{-1} cm^{-1}]	$\lambda_{\text{max,ems}}$ [nm]	Φ	HOMO–LUMO gap [eV] [a]	[b]
1	528	5666	557	0.96	2.29	2.35
2	528		562	0.23	2.27	2.35
3	526	6125	554	0.82	2.29	2.36
4	529	7500	568	0.51	2.25	2.34
5	528	7102	565	0.96	2.27	2.35
6	526	8100	558	0.25	2.29	2.36
7	520	5392	553	1	2.31	2.38

[a] HOMO–LUMO gap calculated from the intersection point of the absorbance and florescence spectra. [b] HOMO–LUMO gap calculated from the λ_{max} of the absorbance spectra.

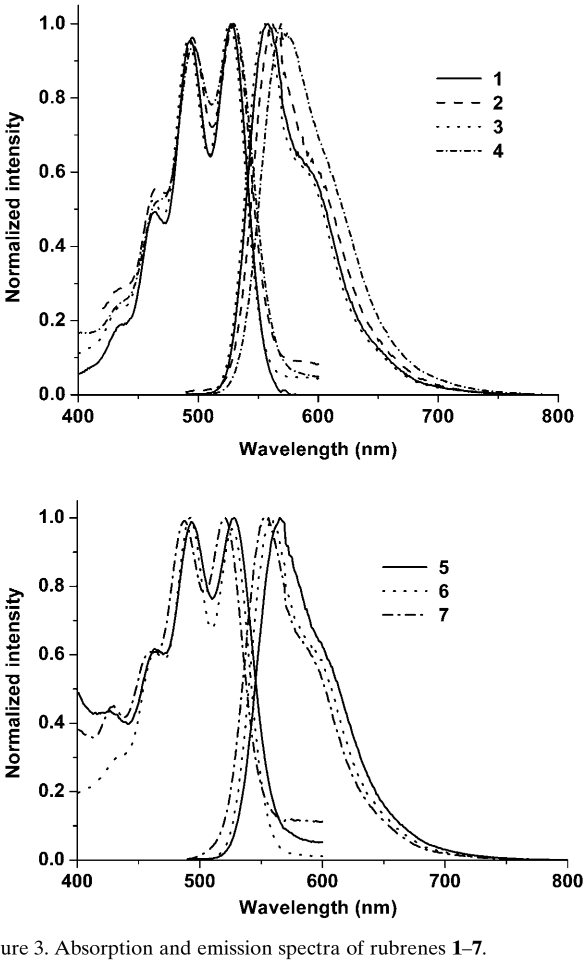

Figure 3. Absorption and emission spectra of rubrenes **1**–**7**.

low, in the range of 23 to 25%. On the other hand, rubrene with methoxy-substitution on the tetracene core (**7**) gives a quantum yield of 100%. For rubrenes with substituents such as F and CN (**3** and **5**), the quantum yield is 82–96%. The extinction coefficients of all rubrene analogues are in the range of 5400 to 8100 $\mathrm{M^{-1}cm^{-1}}$, which is similar to the extinction coefficient of the parent rubrene.[27] The optical HOMO–LUMO gaps calculated from the λ_{max} of the absorbance spectra are in the range of 2.34 to 2.38 eV, whereas those calculated from the intersection point of the absorbance and fluorescence spectra for all rubrenes are in the range of 2.25 to 2.31 eV.

Interestingly, the electronic properties of rubrenes, such as the HOMO–LUMO gap and the absorption and emission spectra, are insensitive to twisting of the tetracene core.[16] Calculated HOMO–LUMO gaps (B3LYP/6-31G(d)) are 2.51 and 2.60 eV, respectively, for C_{2h} symmetry (planar tetracene core) and twisted D_2 symmetry (lowest energy structure) geometries of **1**. The calculated HOMO–LUMO gaps of substituted rubrenes are similar to rubrene **1**, for example, for the twisted (C_1 symmetry) and planar (C_s symmetry) dimethoxy-substituted rubrene **2**, HOMO–LUMO gaps are 2.50 and 2.60 eV, respectively.

Electrochemistry: The electrochemical properties of substituted rubrenes were investigated by cyclic voltammetry (CV; see Table 2, Figure 4, and the Supporting Information). Both the oxidation and reduction processes are reversible for all rubrenes (expect for the reduction of **4**), demonstrating excellent electrochemical stability, and the CV trace does not change under repeated cycling. As expected, the presence of methoxy substituents on the tetracene core results in the $E_{1/2\mathrm{ox}}$ of **7** (0.58 V) being smaller than that of **1** (0.74 V), whereas the $E_{1/2\mathrm{red}}$ (−1.87 V) of **7** is larger than that of **1** (−1.58 V). Methoxy substitution on the phenyl rings (**2**) has little effect on the half-wave potentials (Table 2). The differences between the oxidation and reduction potentials (the electrochemically measured HOMO–LUMO gap) are similar for all of the rubrenes and are in the range of 2.20 to 2.46 V (Table 2).

Table 2. Electrochemical properties of substituted rubrenes.

	$E_{1/2\mathrm{ox}}$ [V]	$E_{1/2\mathrm{red}}$ [V]	$E_{1/2\mathrm{ox}}-E_{1/2\mathrm{red}}$ [eV]
1	0.75	−1.56	2.31
2	0.76	−1.59	2.35
3	0.80	−1.62	2.42
4	0.88	−1.32	2.20
6	0.76	−1.62	2.38
7	0.58	−1.88	2.46

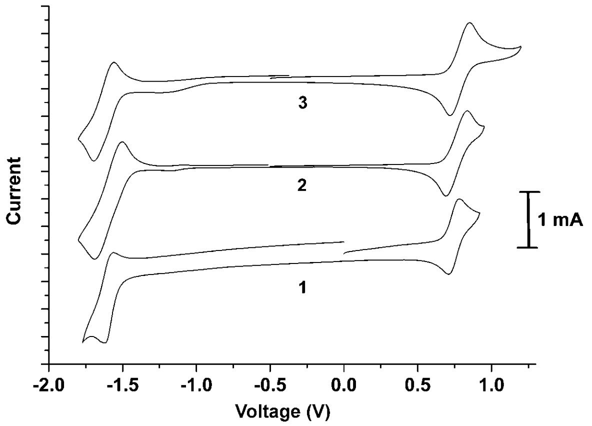

Figure 4. CV traces of **1**–**3** on a platinum electrode versus Ag/AgCl in 1,2-dichloroethane/tetrabutylammonium perchlorate (0.1 M).

Conclusion

We have shown that the planar structure of **1** found in single crystals is due to crystal-packing forces and most substituted rubrenes are not planar in single crystals. Rubrenes (including parent rubrene **1**) also adopt a twisted structure in solution. We have found that the balance between the planar and nonplanar structures of **1** and its derivatives is very delicate and may change as a result of different crystal-packing forces.[28] We have clearly shown that the structure of acene molecules differs between solution and the solid state, and that their planarity is strongly affected by crystal-packing forces. Significant modification of the solid-state structure and properties of rubrenes has been achieved by substitution of peripheral phenyl rings. The fact that **1** shows a high field-effect mobility as single crystals, but has yet to be made into a working thin-film device might be related to the change in its planarity. The high efficiency of rubrene in LED devices might also be associated with its twisted structure.[29] Due to low field-effect mobility in thin films, rubrenes may not be good candidates for use in thin film FETs;[30] however, they are excellent candidates for applications in LEDs. We expect that the substituted rubrenes obtained in this study will have a small tendency to crystallize and will prove to be good candidates for applications in LEDs.

Experimental Section

General: THF and Et_2O were distilled from sodium and benzophenone. Hydroiodic acid was purchased from Aldrich as a 57% aqueous solution stabilized with phosphorous acid. ^1H and ^{13}C NMR spectra were measured at 250 and 400 MHz, respectively, with a Brucker 250 or a Brucker 400 spectrometer. ^1H NMR chemical shifts are reported in parts per million (ppm) relative to tetramethylsilane (0.0 ppm) or chloroform (7.26 ppm). Data are reported as follows: chemical shift, multiplicity (s = singlet, d = doublet, t = triplet, q = quartet, m = multiplet), coupling constants (Hertz), and integration. In ^{13}C NMR spectra sometimes some signals are missing due to poor signal to noise ratio because of poor solubility. Flash chromatography was performed by using silica gel 60 (230–400 mesh). Analytical thin-layer chromatography (TLC) was performed by using 0.25 mm Merck precoated silica gel plates (60-F254). All air- and/or moisture-sensitive reactions were conducted in flame- and/or oven-dried glassware under a dry argon atmosphere with standard precautions taken to exclude moisture. All mass spectrometer measurements were performed with a Micromass platform LCZ 4000 instrument in ESI mode. Elemental analysis was carried out with a FlashEA 1112 Thermo

Finnigan CHN elemental analyzer. Crystals were grown by dissolving rubrenes in CH_2Cl_2 and then adding EtOH until it formed 20 % of the mixture. Crystals were grown in a special desiccator under a constant continuous flow of nitrogen.

Absorption and emission spectroscopy: UV/Vis spectra were obtained on a Jasco 570 spectrophotometer. Fluorescence spectra were recorded on a Varian Cary Eclipse fluorimeter in a 1 cm quartz cuvette with CH_2Cl_2 as the solvent. All measurements were made under a nitrogen atmosphere and the spectrometer was purged with nitrogen for 5 min before each measurement. The quantum efficiency was calculated by using rhodamine B in EtOH (Aldrich) as the reference.

CV measurements: CV measurements were performed with a three-electrode cell in a solution of 0.1 M tetrabutylammonium perchlorate (Bu_4NClO_4) in 1,2-dichloroethane at a scan rate of $100\,mV\,s^{-1}$. All the measurements were performed under an argon atmosphere and before each measurement argon was purged through the solution for 20 min to deoxygenate the system. A Pt wire was used as the counter electrode, Pt was used as the working electrode, and Ag/AgCl was used as the reference electrode. Its potential was corrected to the saturated calomel electrode (SCE) by measuring the ferrocene/ferrocenium couple in this system (0.40 V versus SCE).

DFT calculations: All calculations were performed by using DFT with the B3LYP hybrid functional[31] and the 6-31G(d) basis set. The Gaussian 03 program was used for all computations.[32] Frequency calculations were performed at the same level for all stationary points to define them as minima or saddle points. We note that, in contrast to many ab initio methods (such as MP2, CISD, CCSD), the B3LYP level always yields real frequencies for benzene regardless of the basis set used.[33] The ^{13}C NMR chemical shieldings were calculated by using the gauge-included atomic orbitals (GIAO) method[34] coupled with B3LYP and the 6-311G(2df,p) basis set using the B3LYP/6-31G(d) optimized geometries (these calculations are denoted as GIAO-B3LYP/6-311G(2df,p)//B3LYP/6-31G(d)). The ^{13}C NMR chemical shifts were referenced to TMS, which was calculated at the same level of theory ($\sigma = 182.75$ ppm).

1-(4-Methoxyphenyl)-3-phenylisobenzofuran (9):[35] A solution containing 1-bromo-4-methoxybenzene (4.9 g, 26.3 mmol) was dissolved in THF (75 mL) and cooled to −78 °C, and *n*BuLi (16.5 mL of a 1.6 M solution in hexanes, 26.3 mmol) was added dropwise under an argon atmosphere while maintaining the temperature at below −60 °C. The solution was stirred for 2 h followed by the dropwise addition of a solution of 3-phenylphthalide (5.0 g, 23.7 mmol) in THF (35 mL) over a 45 min period. The deep red solution was stirred for another 15 min at −78 °C. After that, Ac_2O (2.5 mL, 26.5 mmol) was added and the solution was warmed to room temperature and then heating at reflux for 10 min. Water was added to the bright yellow solution and the organic layer was separated and dried over $MgSO_4$ and concentrated. Chromatographic separation (hexane/EtOAc 9:1) gave **9** (1.05 g, 16 %). ^1H NMR (250 MHz, $CDCl_3$): $\delta = 7.95–7.77$ (m, 6 H), 7.45 (t, $J = 8.0$ Hz, 2 H), 7.31–7.27 (m, 1 H), 7.07–6.97 (m, 4 H), 3.89 ppm (s, 3 H); ^{13}C NMR (62.5 MHz, $CDCl_3$): $\delta = 159.7$, 129.9, 127.5, 127.3, 126.1, 125.53, 125.50, 121.2, 121.0, 115.5, 56.4 ppm; MS: *m/z*: 300 $[M]^+$, 301.43 $[M+1]^+$, 323.40 $[M+Na]^+$, 339.38 $[M+K]^+$, 307.42 $[M+Li]^+$, 623.67 $[2M+Na]^+$, 607.70 $[2M+Li]^+$.

6,7-Dimethoxynaphthalene-1,4-dione (10): Compound **10** was prepared according to the procedure described in the literature.[36]

6,11-Diphenyltetracene-5,12-dione (11):[19a] Compound **8** (5 g, 18.5 mmol) was added slowly as a solid to **10** (3 g, 18.9 mmol) in CH_2Cl_2 (50 mL) and the solution was stirred at room temperature for 12 h. Additional CH_2Cl_2 (100 mL) was added and the mixture was cooled to −78 °C followed by dropwise addition of BBr_3 (30 mL of a 1 M solution in CH_2Cl_2, 30 mmol). After 0.5 h at −78 °C, the dark reaction mixture was warmed to room temperature, then heated at reflux for 4 h, and subsequently cooled to room temperature. The solution was then poured into water and the aqueous portion was extracted with CH_2Cl_2. The combined organic extracts were washed with brine, dried ($MgSO_4$), and concentrated in vacuo to give a yellow solid, which was purified by column chromatography (CH_2Cl_2) to give **11** as a bright yellow crystalline solid (7.0 g, 92 %). ^1H NMR ($CDCl_3$, 250 MHz): $\delta = 8.06$ (dd, $J = 3.5$, 6.0 Hz, 2 H), 7.64 (dd, $J = 3.5$, 6.0 Hz, 2 H), 7.59–7.54 (m, 8 H), 7.51–7.47 (m, 2 H), 7.33–7.30 ppm (m, 4 H); ^{13}C NMR (62.5 MHz, $CDCl_3$): $\delta = 184.2$, 144.0, 140.3, 135.6, 134.9, 133.6, 128.9, 128.8, 128.6, 128.4, 127.1, 126.9 ppm.

6-(4-Methoxyphenyl)-11-phenyltetracene-5,12-dione (12): Solid **9** (1.05 g, 3.5 mmol) was slowly added to 1,4-naphthaquinone (0.55 g, 3.5 mmol) dissolved in CH_2Cl_2 (70 mL), and the solution was stirred at room temperature for 12 h. The mixture was cooled to −78 °C followed by the dropwise addition of BBr_3 (4.0 mL of a 1 M solution in CH_2Cl_2, 4.0 mmol). After 1 h at −78 °C, the dark reaction mixture was slowly warmed to room temperature, continuously stirred for another 6 h, then heated at reflux for 4 h, and subsequently cooled to room temperature. The solution was then poured into water and the aqueous portion was extracted with CH_2Cl_2. The combined organic extracts were washed with brine, dried ($MgSO_4$), and concentrated in vacuo to give a yellow solid, which was purified by column chromatography (hexane/EtOAc 3:1) to give **12** as bright yellow crystalline needles (1.33 g, 86 %). ^1H NMR ($CDCl_3$, 250 MHz): $\delta = 8.11–8.06$ (m, 2 H), 7.68–7.48 (m, 8 H), 7.33–7.29 (m, 2 H), 7.25–7.22 (m, 3 H), 7.15–7.11 (m, 2 H), 3.96 ppm (s, 3 H).

2,3-Dimethoxy-6,11-diphenyltetracene-5,12-dione (13): Compound **8** (0.361 g, 1.34 mmol) was added slowly as a solid to **10** (0.291 g, 1.34 mmol) dissolved in CH_2Cl_2 (15 mL) and the solution was stirred at room temperature for 12 h. Additional CH_2Cl_2 (3 mL) was added, and the mixture was cooled to −78 °C followed by dropwise addition of BBr_3 (1.5 mL of a 1 M solution in CH_2Cl_2, 1.5 mmol). After 1 h at −78 °C, the dark reaction mixture was slowly warmed to room temperature, continuously stirred for another 6 h, then heated at reflux for 4 h, and subsequently cooled to room temperature. The solution was then poured into water and the aqueous portion was extracted with CH_2Cl_2. The combined organic extracts were washed with brine, dried ($MgSO_4$), and concentrated in vacuo to give a yellow solid, which was purified by column chromatography (CH_2Cl_2) to give **13** as bright yellow crystalline needles (0.470 g, 82 %). ^1H NMR ($CDCl_3$, 250 MHz): $\delta = 7.62–7.45$ (m, 12 H), 7.32 (d, $J = 2.5$ Hz, 2 H), 7.29 (d, $J = 2.5$ Hz, 2 H), 3.92 ppm (s, 6 H); ^{13}C NMR (100 MHz, $CDCl_3$): $\delta = 183.1$, 153.7, 143.9, 140.7, 135.5, 133.0, 130.6, 129.8, 129.6, 128.7, 128.5, 128.3, 127.0, 108.1, 56.5 ppm; MS: *m/z*: 471 $[M]^+$, 493 $[M+Na]^+$, 510 $[M+K]^+$, 964.30 $[2M+Na]^+$.

5,12-Dihydro-5,12-bis(4-methoxyphenyl)-6,11-diphenyltetracene-5,12-diol (15):[19a] *n*BuLi (6 mL of a 1.6 M solution in hexanes, 9.6 mmol) was added dropwise to a stirred solution of 4-bromoanisole (1.25 mL, 10 mmol) in THF (10 mL) at −78 °C. The mixture was allowed to stir at this temperature for 15 min before being transferred by cannula to a stirred solution of quinone **11** (0.41 g, 1 mmol) in THF (10 mL) at −78 °C. The resulting dark reaction mixture was then allowed to warm to room temperature slowly over a 12 h period and then quenched by pouring into a saturated aqueous solution of NH_4Cl. The aqueous portion was subsequently extracted with Et_2O, and the combined organic extracts were dried ($MgSO_4$) and then concentrated in vacuo to give **15** (0.5 g, 80 %). ^1H NMR (250 MHz, $CDCl_3$): $\delta = 7.71$ (dd, $J = 3.0$, 5.3 Hz, 2 H), 7.56 (q, $J = 3.2$ Hz, 2 H), 7.48 (d, $J = 8.7$ Hz, 4 H), 7.32–7.28 (m, 2 H), 7.25–7.19 (m, 10 H), 6.97–6.94 (m, 2 H), 6.58 (d, $J = 8.7$ Hz, 4 H), 3.74 ppm (s, 6 H); ^{13}C NMR (62.5 MHz, $CDCl_3$): $\delta = 158.8$, 150.2, 144.8, 137.0, 132.1, 131.9, 131.1, 130.0, 129.9, 127.8, 127.4, 127.0, 126.3, 126.0, 125.8, 122.5, 113.0, 55.2 ppm.

5,12-Bis(4-fluorophenyl)-5,12-dihydro-6,11-diphenyltetracene-5,12-diol (16): A dry argon flushed 50 mL flask equipped with magnetic stirrer and a septum was charged with *i*PrMgCl·LiCl[20] (6 mL of a 1 M solution in THF, 6 mmol). The reaction mixture was cooled to −15 °C and 4-fluorobromobenzene (1.05 g, 6 mmol) was added in one portion. The temperature of the reaction mixture was raised to −10 °C and the Br/Mg exchange was completed after 15 min. In another flask, quinone **11** (0.410 g, 1 mmol) was dissolved in THF (10 mL) and the reaction mixture was cooled at −78 °C. a solution of Grignard reagent was added dropwise to this solution through a cannula at −78 °C. The resulting dark reaction mixture was allowed to stir at this temperature for 3 h and then allowed to warm to room temperature slowly over a 12 h period. It was then quenched by pouring the mixture into a saturated aqueous solution of NH_4Cl. The aqueous portion was subsequently extracted with Et_2O, and the combined organic extracts were dried ($MgSO_4$) and then concentrated in vacuo. The resulting white solid was washed to obtain pure diol **16**

(0.250 g, 42 %). ^{1}H NMR (250 MHz, $CDCl_3$): $\delta = 7.25$–7.17 (m, 8H), 7.01–6.94 (m, 12H), 6.77–6.70 (m, 4H), 6.19 (d, $J = 7.7$ Hz, 2H), 3.91 ppm (s, 2H); ^{13}C NMR (62.5 MHz, $CDCl_3$): $\delta = 162.9$, 159.0, 145.3, 145.3, 141.0, 139.6, 137.3, 136.4, 134.4, 131.6, 131.2, 128.8, 127.6, 127.3, 127.1, 127.1, 126.9, 126.6, 126.3, 126.2, 114.3, 113.4, 74.8 ppm.

5,12-Bis(4-(diethoxymethyl)phenyl)-5,12-dihydro-6,11-diphenyltetracene-5,12-diol (17): Dry THF (10 mL) and *n*BuLi (3 mL of a 1.6 M solution in hexane, 4.8 mmol) were added sequentially to a 50 mL two-necked flask equipped with a stirring bar under N_2 at −78 °C. 4-Bromobenzaldehyde diethyl acetal (0.976 mL, 4.8 mmol) was then added to this solution and the mixture was stirred at −78 °C for 3 h. The mixture was slowly warmed to room temperature and then cooled again to −78 °C before the addition of quinone **11** (0.205 g, 0.5 mmol) dissolved in THF (10 mL). The resulting dark reaction mixture was allowed to stir at this temperature for 1 h and then allowed to warm to room temperature slowly over a 12 h period. It was then quenched by pouring the mixture into a saturated aqueous solution of NH_4Cl. The aqueous portion was subsequently extracted with Et_2O, and the combined organic extracts were dried ($MgSO_4$) and then concentrated in vacuo. The resulting white solid was purified by column chromatography with CH_2Cl_2/EtOAc (10:1) as the eluent to give diol **17** (0.37 g, 98 %). ^{1}H NMR (250 MHz, $CDCl_3$): $\delta =$ 7.60–7.51 (m, 2H), 7.42–7.38 (m, 5H), 7.30–7.28 (m, 2H), 7.17–6.89 (m, 16H), 6.12 (d, $J = 7.7$, Hz, 1H), 5.43 (s, 2H), 3.80 (s, 1H), 3.66–3.50 (m, 8H), 2.04 (s, 1H), 1.29–1.18 (m, 12H); MS: *m*/*z*: $[M]^+$ 770, $[M{+}Na]^+$ 794.11; $[M{+}K]^+$ 810.05.

5,12-Bis(4-fluorophenyl)-5,12-dihydro-6-(4-methoxyphenyl)-11-phenyltetracene-5,12-diol (19): *n*BuLi (4.05 mL of a 1.6 M solution in hexane, 6.48 mmol) was added dropwise to a solution of 1-bromo-4-fluorobenzene (0.75 mL, 6.83 mmol) in THF (10 mL) at −78 °C while stirring for 1 h. A solution of quinone **12** (0.300 g, 0.683 mmol) dissolved in THF (15 mL) was then added to this solution. The resulting dark reaction mixture was stirred at this temperature for 1 h and then allowed to warm to room temperature over a 12 h period with continuous stirring. The reaction mixture was quenched by pouring into a saturated aqueous solution of NH_4Cl. The aqueous portion was subsequently extracted with Et_2O, and the combined organic extracts were dried ($MgSO_4$) and then concentrated in vacuo. Column chromatography with hexane/EtOAc (3:1) as the eluent gave **19** (0.140 g, 33 %). ^{1}H NMR (250 MHz, $CDCl_3$): $\delta = 7.70$ (dd, $J = 3.0$, 8.5 Hz, 2H), 7.59–7.53 (m, 4H), 7.25–7.21 (m, 4H), 7.04–6.94 (m, 6H), 6.79–6.70 (m, 6H), 6.01 (d, $J = 8.2$ Hz, 1H), 5.91 (dd, $J = 2.0$, 6.5 Hz, 1H), 3.82 (s, 3H), 3.80 (s, 1H), 3.64 ppm (s, 1H); MS: *m*/*z*: 632 $[M]^+$, 631.53 $[M{-}1]^+$, 667.43 $[M{-}1{+}Cl]^+$, 745.23 $[M{-}1{+}TFA]^+$, 655.61 $[M{+}Na]^+$.

5,12-Dihydro-2,3-dimethoxy-5,6,11,12-tetraphenyltetracene-5,12-diol (20): Dimethoxy quinone **13** (0.470 g, 1.1 mmol) was dissolved in THF (15 mL) and the reaction mixture was cooled to −78 °C. PhLi (3 mL of a 1.8 M solution in dibutyl ether, 5.4 mmol) was added dropwise to this solution. The resulting dark reaction mixture was stirred at this temperature for 1 h and then allowed to warm to room temperature slowly over a 12 h period. The reaction was then quenched by pouring the mixture into an aqueous solution of saturated NH_4Cl. The aqueous portion was subsequently extracted with Et_2O, and the combined organic extracts were dried ($MgSO_4$) and then concentrated in vacuo. The resulting pale-yellow solid was purified by column chromatography with CH_2Cl_2/EtOAc (20:1) as the eluent to give two isomers of diol **20** (0.218 g, 35 %). Isomer A: ^{1}H NMR (250 MHz, $CDCl_3$): $\delta = 7.65$–7.54 (m, 2H), 7.45–7.33 (m, 2H), 7.19–7.02 (m, 14H), 6.97–6.93 (m, 2H), 6.89–6.83 (m, 2H), 6.55 (s, 2H), 6.19–6.15 (m, 2H), 3.90 (s, 2H), 3.58 ppm (s, 6H). Isomer B: ^{1}H NMR (250 MHz, $CDCl_3$): $\delta = 7.34$–7.32 (m, 4H), 7.18–7.03 (m, 14H), 6.96–6.92 (m, 2H), 6.88–6.82 (m, 2H), 6.52 (s, 2H), 6.17–6.14 (m, 2H), 3.61 (s, 2H), 3.57 ppm (s, 6H); MS: *m*/*z*: 627 $[M]$, 650.10 $[M{+}Na]^+$, 1276.96 $[2M{+}Na]^+$, 625.86 $[M{-}1]$, 1252.80 $[2M{-}1]$.

General procedure for the synthesis of compounds 2–7: The diol (0.50 mmol) was dissolved in Et_2O (30 mL) in a 100 mL flask under N_2 with heating. 57 % aqueous HI (6 mL) was then added to this solution at reflux. The reaction was allowed to proceed for 10 min and cooled to room temperature and then aqueous saturated sodium metabisulfite (20 mL) was added to form a red ether layer. The organic layer was separated, immediately dried over $MgSO_4$, and concentrated. Immediate flash chromatography (CH_2Cl_2-hexane) followed by sublimation gave rubrenes (**2**–**7**) as red solids. The yields were determined after flash chromatography.

*5,12-Bis(4-methoxyphenyl)-6,11-diphenyltetracene (**2**)*:[19a] Red solid; yield = 62 %; ^{1}H NMR (250 MHz, $CDCl_3$): $\delta = 7.76$ (dd, $J = 3.2$, 7.0 Hz, 2H), 7.64 (dd, $J = 3.2$, 7.0 Hz, 2H), 7.04–6.88 (m, 14H), 6.79 (dd, $J = 1.8$, 8.5 Hz, 4H), 6.53 (dd, $J = 2.5$, 7.0 Hz, 4H), 3.41 ppm (s, 6H); MS: 592 $[M]^+$, 590.99 $[M{-}1]^+$, 615.13 $[M{+}Na]^+$, 631.27 $[M{+}K]^+$, 1223.39 $[2M{+}K]^+$; elemental analysis calcd (%) for $C_{44}H_{32}O_2$: C 89.16, H 5.44; found: C 89.02, H 4.34.

*5,12-Bis(4-fluorophenyl)-6,11-diphenyltetracene (**3**)*: Red solid; yield = 96 %; ^{1}H NMR (250 MHz, $CDCl_3$): $\delta = 7.77$–7.71 (m, 2H), 7.59–7.55 (m, 2H), 7.39–7.32 (m, 4H), 7.22 (d, $J = 2.7$ Hz, 2H), 7.19–6.90 (m, 8H), 6.89–6.72 ppm (m, 8H); ^{13}C NMR (62.5 MHz, $CDCl_3$): $\delta = 163.2$, 159.3, 141.8, 138.4, 133.4, 133.3, 131.9, 130.6, 130.4, 127.3, 126.4, 126.1, 126.0, 124.7, 124.5, 122.4, 114.2, 114.0 ppm; elemental analysis calcd (%) for $C_{42}H_{26}F_2$: C 88.71, H 4.61; found: C 88.68, H 4.55.

*5,12-Bis(4-carboxyaldhydephenyl)-6,11-diphenyltetracene (**4**)*: Red solid; yield = 79 %;. ^{1}H NMR (250 MHz, $CDCl_3$): $\delta = 10.02$ (s, 2H), 7.68–7.54 (m, 6H), 7.40–7.33 (m, 3H), 7.30–7.28 (m, 2H), 7.24–7.01 (m, 12H), 6.88–6.83 ppm (m, 3H); ^{13}C NMR (62.5 MHz, $CDCl_3$): $\delta = 192.2$, 192.0, 148.6, 141.2, 136.8, 136.1, 134.1, 132.7, 132.5, 130.6, 129.6, 128.6, 127.4, 126.5, 126.4, 126.0, 125.5 ppm; MS: m/z: 589 $[M]^+$, 611.83 $[M{+}Na]^+$, 627.91 $[M{+}K]^+$; elemental analysis calcd (%) for $C_{44}H_{28}O_2$: C 89.77, H 4.79; found: C 89.58, H 4.65.

*5,12-Bis(4-cyanophenyl)-6,11-diphenyltetracene (**5**)*: Red solid; ^{1}H NMR (250 MHz, $CDCl_3$): $\delta = 7.41$–7.35 (m, 6H), 7.24–7.10 (m, 12H), 7.03–6.97 (m, 4H), 6.90–6.86 ppm (m, 4H); ^{13}C NMR (62.5 MHz, $CDCl_3$): $\delta =$ 146.7, 141.2, 136.6, 135.5, 132.6, 132.4, 130.9, 130.7, 129.5, 128.4, 128.2, 127.6, 127.2, 126.6, 126.4, 125.8, 125.7, 109.6 ppm.

*5,12-Bis(4-fluorophenyl)-6-(4-methoxyphenyl)-11-phenyltetracene (**6**)*: Red crystals; yield = 43 %; ^{1}H NMR (250 MHz, $CDCl_3$): $\delta = 7.46$–7.42 (m, 1H), 7.38–7.31 (m, 3H), 7.18–7.09 (m, 7H), 6.89–6.74 (m, 12H), 6.72–6.66 (m, 2H), 3.87 ppm (s, 3H); ^{13}C NMR (62.5 MHz, $CDCl_3$): $\delta = 158.0$, 141.8, 134.2, 133.5, 133.4, 133.3, 133.2, 133.0, 130.3, 127.3, 126.6, 126.5, 126.3, 126.0, 125.0, 114.3, 114.2, 114.0, 113.9, 133.4, 112.9, 55.4 ppm; MS: *m*/*z*: 599 $[M]^+$, 599.65 $[M{+}1]^+$, 621.62 $[M{+}Na]^+$, 637.66 $[M{+}K]^+$, 1220.26 $[2M{+}Na]^+$.

*2,3-Dimethoxy-5,6,11,12-tetraphenyltetracene (**7**)*: Red solid; yield = 94 %; ^{1}H NMR (250 MHz, $CDCl_3$): $\delta = 7.37$–7.31 (m, 2H), 7.14–7.01 (m, 14H), 6.89–6.84 (m, 8H), 6.52 (s, 2H), 3.59 ppm (s, 6H); ^{13}C NMR (100 MHz, $CDCl_3$): $\delta = 149.6$, 142.2, 141.9, 136.3, 134.5, 132.2, 131.8, 129.7, 128.6, 127.8, 127.3, 127.1, 126.5, 125.6, 124.4, 102.8, 55.3 ppm; MS: *m*/*z*: 592 $[M]^+$, 593.11 $[M{+}1]^+$.

Acknowledgements

The authors are grateful to Prof. Dmitrii F. Perepichka (McGill University, Canada) and to Prof. Robert Pascal, Jr. (Princeton University) for useful suggestions, to Alex Banaru for helpful discussions and help with X-ray structures, to Elijah Shirman for help with florescence measurements and to Natalia Zamoshchik for help with XRD measurements. We thank the Israel Science Foundation and the Helen and Martin Kimmel Center for Molecular Design for financial support. M.B. is the incumbent of the Recanati career development chair, a member ad personam of the Lise Meitner-Minerva Center for Computational Quantum Chemistry, and the holder of a DuPont Young Professor Award.

---

[1] M. Charles, D. Charles, P. M. Dean, *Compt. Rend.* **1926**, *182*, 1440–1443.

[2] a) E. A. Chandross, J. W. Longworth, R. E. Visco, *J. Am. Chem. Soc.* **1965**, *87*, 3259–3260; b) D. M. Hercules, *Acc. Chem. Res.* **1969**, *2*, 301–307; c) M. M. Richter, *Chem. Rev.* **2004**, *104*, 3003–3036, and references therein.

[3] a) H. E. Katz, Z. Bao, *J. Phys. Chem. B* **2000**, *104*, 671–678; b) C. D. Dimitrakopoulos, P. R. L. Malenfant, *Adv. Mater.* **2002**, *14*, 99; c) M. Bendikov, F. Wudl, D. F. Perepichka, *Chem. Rev.* **2004**, *104*, 4891; d) J. E. Anthony, *Angew. Chem.* **2008**, *120*, 460–492; *Angew. Chem. Int. Ed.* **2008**, *47*, 452–483.

[4] V. C. Sundar, J. Zaumseil, V. Podzorov, E. Menard, R. L. Willett, T. Someya, M. E. Gershenson, J. A. Rogers, *Science* **2004**, *303*, 1644.

[5] J. Takeya, M. Yamagishi, Y. Tominari, R. Hirahara, Y. Nakazawa, T. Nishikawa, T. Kawase, T. Shimoda, S. Ogawa, *Appl. Phys. Lett.* **2007**, *90*, 102120.

[6] The stability of **1** in FET devices has also been studied recently, see: R. Zeis, C. Besnard, T. Siegrist, C. Schlockermann, X. Chi, C. Kloc, *Chem. Mater.* **2006**, *18*, 244–248.

[7] F. Cicoira, J. A. Miwa, D. F. Perepichka, F. Rosei, *J. Phys. Chem. A* **2007**, *111*, 12674–12678.

[8] N. Stingelin-Stutzmann, E. Smits, H. Wondergem, C. Tanase, P. Blom, P. Smith, D. de Leeuw, *Nat. Mater.* **2005**, *4*, 601.

[9] a) A. L. Briseno, S. C. B. Mannsfeld, M. M. Ling, S. Liu, R. J. Tseng, C. Reese, M. E. Roberts, Y. Yang, F. Wudl, Z. Bao, *Nature* **2006**, *444*, 913–917; b) A. L. Briseno, R. J. Tseng, M. M. Ling, E. H. L Falcao, Y. Yang, F. Wudl, Z. Bao, *Adv. Mater.* **2006**, *18*, 2320–2324.

[10] Ambipolar behavior for rubrene-based FETs was also demonstrated, see: T. Takahashi, T. Takenobu, J. Takeya, Y. Iwasa, *Appl. Phys. Lett.* **2006**, *88*, 33505.

[11] See also C. H. Hsu, J. Deng, C. R. Staddon, P. Beton, *Appl. Phys. Lett.* **2007**, *91*, 193505.

[12] D. A. da Silva Filho, E.-G. Kim, J.-L. Brédas, *Adv. Mater.* **2005**, *17*, 1072.

[13] I. Bulgarovskaya, V. Vozzhennikov, S. Aleksandrov, V. Bel'skii, *Latv. PSR Zinat. Akad. Vestis Kim. Ser.* **1983**, *4*, 53. The same unit cell parameters were reported by a) D. E. Henn, W. G. Williams, D. J. Gibbons, *J. Appl. Crystallogr.* **1971**, *4*, 256; b) O. D. Jurchescu, A. Meetsma, T. T. M. Palstra, *Acta Crystallogr. Sect. B* **2006**, *62*, 330–334.

[14] R. A. Pascal, Jr., *Chem. Rev.* **2006**, *106*, 4809–4819.

[15] On the other hand, the rubrene cation radical has a 27° twist (M. Kameya, T. Naito, T. Inabe, *Bull. Chem. Soc. Jpn.* **2000**, *73*, 61) and complexation of the four phenyl groups of rubrene with very bulky RuCp* (Cp = cyclopentadienyl) groups results in a twist of 69° (P. J. Fagan, M. D. Ward, J. V. Caspar, J. C. Calabrese, P. J. Krusic, *J. Am. Chem. Soc.* **1988**, *110*, 1981–1983).

[16] J. E. Norton, K. N. Houk, *J. Am. Chem. Soc.* **2005**, *127*, 4162–4163.

[17] This is contrast to other conjugated systems, such as oligothiophenes, in which very little twisting energy is required to achieve a significant change in HOMO–LUMO gap, see: S. S. Zade, M. Bendikov, *Chem. Eur. J.* **2007**, *13*, 3688–3700.

[18] a) M.-C. Blüm, E. Ćavar, M. Pivetta, F. Patthey, F.-D. Schneider, *Angew. Chem.* **2005**, *117*, 5468–5471; *Angew. Chem. Int. Ed.* **2005**, *44*, 5334–5337; b) D. Käfer, G. Witte, *Phys. Chem. Chem. Phys.* **2005**, *7*, 2850–2853; c) M.-C. Blüm, M. Pivetta, F. Patthey, F.-D. Schneider, *Phys. Rev. B* **2006**, *73*, 195409; d) D. Käfer, L. Ruppel, G. Witte, Ch. Wöll, *Phys. Rev. Lett.* **2005**, *95*, 166602.

[19] a) J. A. Dodge, J. D. Bain, A. R. Chamberlin, *J. Org. Chem.* **1990**, *55*, 4190, and references therein; b) Y. S. Wu, T. H. Liu, H. H. Chen, C. H. Chen, *Thin Solid Films* **2006**, *496*, 626.

[20] A. Krasovskiy, P. Knochel, *Angew. Chem.* **2004**, *116*, 3396–3399; *Angew. Chem. Int. Ed.* **2004**, *43*, 3333–3336.

[21] While this work was completed and prepared for publication, an X-ray structure of a different twisted rubrene (5,11-bis-4-*tert*-butylphenyl-6,12-diphenylnaphthacene) was reported, see: S. Haas, A. F. Stassen, G. Schuck, K. P. Pernstich, D. J. Gundlach, B. Batlogg, U. Berens, H.-J. Kirner. *Phys. Rev. B* **2007**, *76*, 115203.

[22] a) R. P. L'Esperance, D. V. Engen, R. Dayal, R. A. Pascal, Jr., *J. Org. Chem.* **1991**, *56*, 688–694; b) D. D. MacNicol, P. R. Mallinson, C. D. Robertson, *J. Chem. Soc. Chem. Commun.* **1985**, 1649–1651.

[23] See the Supporting Information for details.

[24] A similar structure was also reported in references [7] and [18b].

[25] Interestingly, by using the default conditions in Gaussian 03, the C_{2h}-symmetry structure of **1** (as well as of all other rubrenes) has one imaginary frequency and can be formally characterized as a saddle point. However, more careful examination has shown that this saddle point connects two minima of C_2 symmetry, which are geometrically and energetically undistinguishable from C_{2h} structure. So, most probably, the imaginary frequency in the C_{2h} structure is a computational artefact, and such a structure might be a true minimum on the potential-energy surface.

[26] The ^{13}C NMR chemical shift of benzene calculated at the GIAO-B3LYP/6-311G(2df,p)//B3LYP/6-31G(d) level is $\delta = 133.25$ ppm, whereas the experimental value is $\delta = 128.0$ ppm. Therefore, such a calculation systematically overestimates the ^{13}C NMR chemical shifts of aromatic carbon atoms by 5.25 ppm, since the B3LYP method apparently does not include sufficient electron correlation to correctly describe the chemical shifts of aromatic carbon atoms (see: a) J. Gauss, *Chem. Phys. Lett.* **1992**, *191*, 614; b) J. Gauss, *Chem. Phys.* **1993**, *99*, 3629; c) J. J. Buffy, R. West, M. Bendikov, Y. Apeloig, *J. Am. Chem. Soc.* **2001**, *123*, 978–979). If a correction of only 5.25 ppm is applied then the agreement between the experimental values of the twisted conformation is still significantly better than for planar rubrene. The average difference between the measured NMR chemical shifts of the carbon atoms of the tetracene core and the shifts calculated for a twisted conformation is 1.0 ppm, and for planar rubrene it is 2.8 ppm. Calculated values for carbon atoms 5a and 11a in a twisted conformation are 1.2 ppm off the measured values, whereas the difference between the experimental and calculated values is 3.1 ppm for a planar conformation.

[27] a) A. P. Darmanyan, *Izv. Akad. Nauk SSSR* **1982**, *8*, 1888–1891; b) J. W. Arbogast, C. S. Foote, *J. Am. Chem. Soc.* **1991**, *113*, 8886–8889.

[28] We note that, in agreement with our results, in recent STM investigations of the self-assembly of **1** on Au(111), a twisted tetracene core was assumed for **1**.[18]

[29] Usually, good solid-state packing is required for applications in FETs, whereas weak intramolecular interactions are required for applications in LEDs. Rubrene (**1**) was used in LEDs, which suggests weak intermolecular interactions, on the other hand, crystals of **1** show high field-effect mobility (and consequently strong intermolecular interactions). This apparent discrepancy also supports the conclusion that **1** adopts a different structure as a single crystal than as a thin film.

[30] Recently, high field-effect mobility in rubrene films was obtained by crystallization of amorphous islands of the rubrene film, see ref. [11]; this supports our conclusion that crystallization changes the structure of **1** significantly.

[31] a) R. G. Parr, W. Yang, *Density Functional Theory of Atoms and Molecules*, Oxford University Press, New York, **1989**; b) W. Koch, M. C. Holthausen, *A Chemist's Guide to Density Functional Theory*, Wiley-VCH, Weinheim, **2000**; c) C. Lee, W. Yang, R. G. Parr, *Phys. Rev. B* **1988**, *37*, 785–789; d) A. D. Becke, *J. Chem. Phys.* **1993**, *98*, 5648–5652.

[32] Gaussian 03 (Revision C.02), M. J. Frisch, G. W. Trucks, H. B. Schlegel, G. E. Scuseria, M. A. Robb, J. R. Cheeseman, J. A. Montgomery, Jr., T. Vreven, K. N. Kudin, J. C. Burant, J. M. Millam, S. S. Iyengar, J. Tomasi, V. Barone, B. Mennucci, M. Cossi, G. Scalmani, N. Rega, G. A. Petersson, H. Nakatsuji, M. Hada, M. Ehara, K. Toyota, R. Fukuda, J. Hasegawa, M. Ishida, T. Nakajima, Y. Honda, O. Kitao, H. Nakai, M. Klene, X. Li, J. E. Knox, H. P. Hratchian, J. B. Cross, C. Adamo, J. Jaramillo, R. Gomperts, R. E. Stratmann, O. Yazyev, A. J. Austin, R. Cammi, C. Pomelli, J. W. Ochterski, P. Y. Ayala, K. Morokuma, G. A. Voth, P. Salvador, J. J. Dannenberg, V. G. Zakrzewski, S. Dapprich, A. D. Daniels, M. C. Strain, O. Farkas, D. K. Malick, A. D. Rabuck, K. Raghavachari, J. B. Foresman, J. V. Ortiz, Q. Cui, A. G. Baboul, S. Clifford, J. Cioslowski, B. B. Stefanov, G. Liu, A. Liashenko, P. Piskorz, I. Komaromi, R. L. Martin, D. J. Fox, T. Keith, M. A. Al-Laham, C. Y. Peng, A. Nanayakkara, M. Challacombe, P. M. W. Gill, B. Johnson, W. Chen, M. W. Wong, C. Gonzalez, J. A. Pople, Gaussian, Inc., Pittsburgh, PA, **2003**.

[33] D. Moran, A. C. Simmonett, F. E. Leach III, W. D. Allen, P. v. R. Schleyer, H. F. Schaefer III, *J. Am. Chem. Soc.* **2006**, *128*, 9342.

[34] a) R. Ditchfield, *Mol. Phys.* **1974**, *27*, 789; b) K. Wolinski, J. F. Hinton, P. Pulay, *J. Am. Chem. Soc.* **1990**, *112*, 8251; c) J. R. Cheeseman, G. W. Trucks, T. A. Keith, M. J. Frisch, *J. Chem. Phys.* **1996**, *104*, 5497.

[35] Y. Kuninobu, Y. Nishina, C. Nakagawa, K. Takai, *J. Am. Chem. Soc.* **2006**, *128*, 12376–12377.

[36] J. Reichwagen, H. Hopf, A. D. Guerzo, C. Belin, H. Bouass-Laurent, J.-P. Desvenergne, *Org. Lett.* **2005**, *7*, 971.

Received: April 27, 2008